ELSEVIER

Earth and Planetary Science Letters 142 (1996) 573–585

EPSL

Fault re-activation, stress interaction and rupture propagation of the 1981 Corinth earthquake sequence

Aurélia Hubert [a,*], Geoffrey King [a], Rolando Armijo [a], Bertrand Meyer [a], Dimitri Papanastasiou [b]

[a] *Equipe Sismotectonique et Laboratoire Tectonique, URA 1093, CNRS, Institut de Physique du Globe, 4 place Jussieu 75252, Paris Cedex 05, France*

[b] *National Observatory of Athens, PO Box 20048, 11810 Athens, Greece*

Received 6 December 1995; accepted 28 May 1996

Abstract

By modelling vertical motions associated with the first two events of the 1981 Corinth sequence we show that both events produced surface rupture on the Perahora peninsula, moving in turn the Pisia and Alepohori faults. Motion on an offshore fault, suggested previously, did not occur in 1981, although the fault may have been responsible for the destructive 1928 Corinth event. The data used for the modelling are the most recent estimates of the seismic moments and stress drops of the earthquakes, together with a new information about coastal uplift and subsidence. Identification of the faults and their approximate coseismic slip distributions allows the Coulomb stress interaction between the events to be examined. At a depth of 6 km the rupture surface of the second event, which occurred 4 h after the first, was subject to a Coulomb stress increase of about 30% of its coseismic stress drop. The Coulomb stress on the rupture surface of the third event, which occurred 7 days later, was increased by a more modest 6% of its stress drop. The third event apparently propagated from east to west, consistent with the modelling, which suggests that the largest increase in Coulomb stress occurred at its eastern end. Although the offshore fault did not move in the earthquake sequence, it was bought more than 5 bars closer to failure by the 1981 earthquake sequence, so that future motion on it presents a potential hazard.

Keywords: Corinth Greece; earthquake; faults; stress drops; rupture; models

1. Introduction

In 1981 a sequence of three earthquakes with magnitudes greater than 6 struck the eastern Gulf of Corinth. The first two (Mb 6.7 and 6.4) occurred during the night of the 24th–25th February and the third (Mb 6.3) 7 days later on the 4th of March. North dipping surface breaks (Fig. 1) were noted the morning after the first two events on the southern side of the Gulf and south dipping ruptures appeared on the northern side of the Gulf as a result of the third event [1].

Since the first two events occurred at night it was not clear whether both or only one of them was responsible for the observed north dipping rupture and this problem has remained, despite extensive subsequent work [1–4]. In this paper we show that a

* Corresponding author. E-mail: hubert@ipgp.jussieu.fr

PII S0012-821X(96)00108-2

critical re-examination of the reported sea level changes, combined with modelling vertical deformation can resolve this problem. The faults causing the first two events can be identified. Furthermore, it can be shown that the Coulomb stress changes resulting from the first event might be expected to trigger the second and the combined Coulomb stresses of the first two could have triggered the third.

2. Background

Fig. 1 shows major active faults in the region of the 1981 earthquake sequence [1,5] with those which exhibited surface rupture in 1981 being indicated by more solid lines. Jackson et al. [1] mapped the surface rupture and found offsets of up to 1.5 m on the Pisia fault, 1 m on the Alepohori fault and 1 m

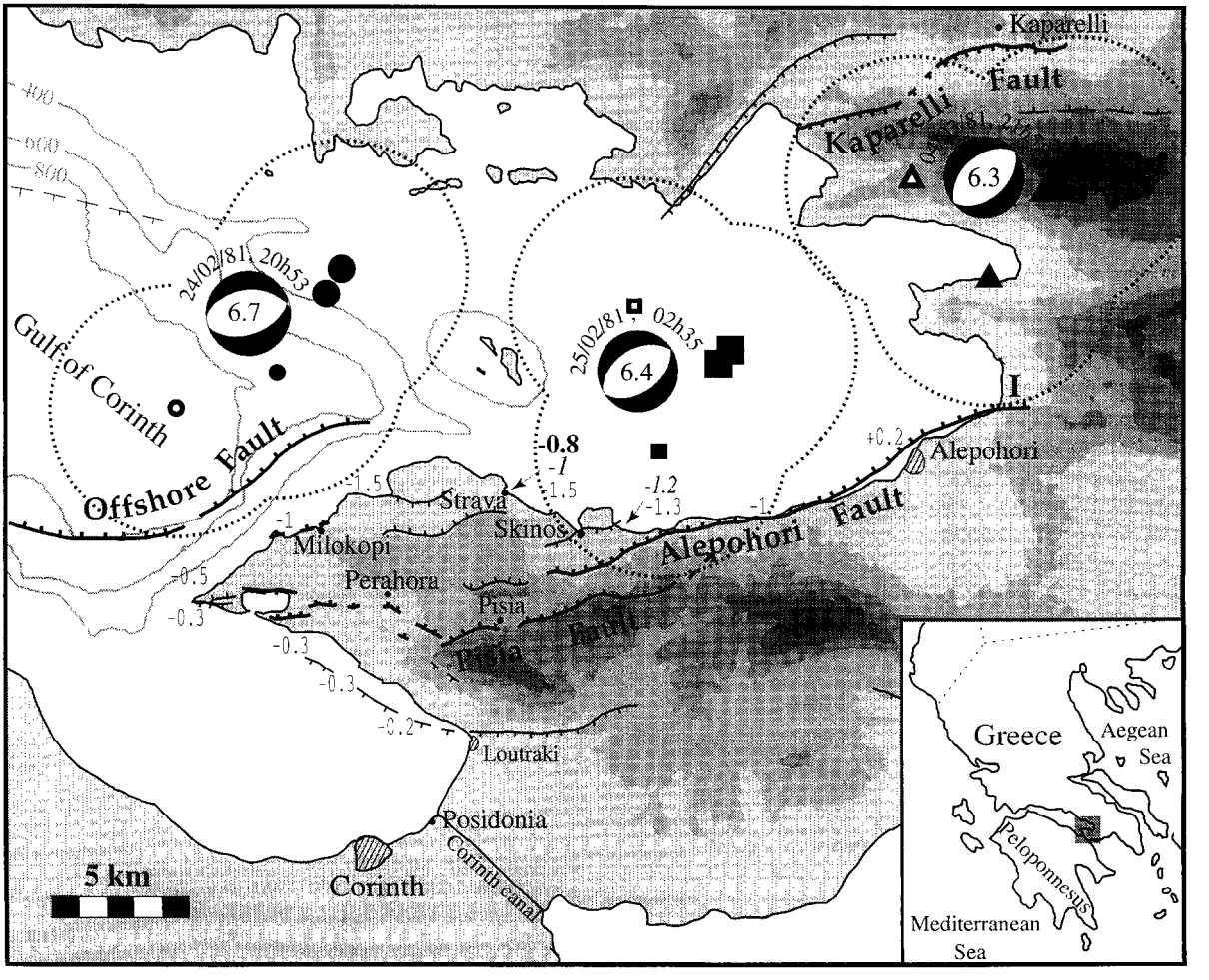

Fig. 1. The epicentral region of the 1981 Gulf of Corinth earthquake sequence. Significant faults are shown, with those known to have moved in 1981 indicated by bold lines. Possible epicentres are indicated by dots, squares and triangles for the 24th February, 25th February and 4th March events, respectively (open symbols from [1]; solid symbols from [3]). The big solid symbols are the locations most favoured by Taymaz et al. [3] and appear in Fig. 7. Quoted location errors associated with the events are thought to be about 5 km, as indicated by dotted lines [3]. Uplift around the coast is indicated: normal type corresponds to the results of Vita-Finzi and King [7], italics to those of Khoury et al. [8] and bold type to this study. The topographic shading increases in intensity every 300 m.

on the Kaparelli fault. Also shown are four possible epicentre locations for each event, with circles indicating likely error based on relative relocation [1,3]. Taymaz et al. [3] argue that the two possibilities indicated by solid symbols are more likely than the others and further note that they both fall on the down-dip projection of the surface breaks. They are also the most consistent with the rupture scenario we suggest later. Based on Table 1, we take mean seismic moments to be 8.8×10^{18} N · m for the first shock, 4.0×10^{18} N · m for the second and 1.9×10^{18} N · m for the third. Uncertainties in these values could be large. Moments could be twice or half of the above values. However, since the moments of all of the events were determined with similar sets of seismic stations and similar ray paths, it is unlikely that errors in relative moments could be that great.

The relation between the third event and the surface breaks on the fault near to Kaparelli was obvious. It occurred 1 week after the first two and the surface breaks appeared at that time. The relative locations of the surface breaks and the probable epicentres are also consistent (Fig. 1). By contrast, the relationship between the first two events and faulting on the Pisia and Alepohori faults is not obvious. Two possibilities have been suggested [1,3]. The first is that the main shock occurred on an offshore fault west of the Perahora peninsula and that the second event produced all the onshore faulting [1]. The second hypothesis is that both of the first two events contributed to the faulting on the Perahora peninsula, with the Pisia fault moving during the first event and the Alepohori fault moving during the second [3]. A third possibility, that our later modelling will exclude, is that the first event occurred on a south dipping antithetic fault.

The seismological information, including the aftershock distribution [6] and the surface rupture, are insufficient to distinguish between the different possibilities. Observations of uplift and subsidence relative to sea level together with deformation modelling, however, can be used to provide further information. In Fig. 1 various estimates of the coseismic changes of sea level are shown around the Perahora peninsula based on the work of Vita-Finzi and King [7] and Khoury et al. [8]. Vita-Finzi and King [7] reported changes largely based on the reports of local fishermen who worked all around the coast while Khoury et al. [8] concentrated on the area around Skinos. Some 10 years later Pirazzoli et al. [9] contested the results of Vita-Finzi and King [7] near to Milokopi (Fig. 1) on the grounds that the coastal biological zones showed no significant evidence of long-term perturbation. Thus, subsidence in this region was probably much less than the changes reported by word of mouth.

In June, 1994, we re-examined the region around Strava, north of the Pisia fault (Fig. 1) and discovered further evidence for changes in sea level in the form of geological markers and markers resulting from human activity. The geological evidence is indicated in Fig. 2 where the levels of a submerged beach and a submerged solution notch can be seen. Fig. 3 shows two jetties recently built upon older, now submerged jetties. These have both been raised by 80 cm, a value consistent with the apparent

Table 1
Estimates of the seismic moments for the three events of the 1981 Corinth earthquake

Reference	24th February 1981		25th February 1981		4th March 1981	
	Mo ($\times 10^{18}$ Nm)	$\Delta\sigma$ (bar)	Mo ($\times 10^{18}$ Nm)	$\Delta\sigma$ (bar)	Mo ($\times 10^{18}$ Nm)	$\Delta\sigma$ (bar)
[1]	7.3	34	1.7	7	0.97	5
[20]	12.9		4.3		3.5	
[13]	8.1	10	2.7	8	2.2	7
[21]	10.0		3.5		1.9	
[3]	8.75		3.97		2.70	
[4]	6.0 ± 2.4	22 ± 10	1.5 ± 0.6	13 ± 5	1.3 ± 0.6	16 ± 10
[14]	9.01		3.75		2.8	

subsidence of the features shown in Fig. 2. This should be representative of the subsidence following the event, bearing in mind that there has been no other seismic deformation sources, indeed no major events, since 1928.

The photographs also suggest why the earlier reports of sea level change may have been in error. The two photographs in Fig. 3 show that the sea level changed by 60 cm in 3 days. Even though they were taken near to the time of tidal maximum (new moon) the change is larger than can be readily explained by the maximum lunar–solar tidal range alone (50 cm). Eleven days of tidal record from the gauge at Posidonia (Fig. 4) show a tidal peak to peak amplitude of 50 cm at new and full moon dropping to a few centimetres at half moon. It was on the basis of this small tidal range, giving a maximum error of less than ± 25 cm, that earlier workers considered that its effects could easily be separated from coseismic changes.

Prompted by the observations shown in Fig. 3, subsequent inquiry has shown that secular variations larger than the solar/lunar tides occur and can last for long periods of time. Extreme sea level changes in the period 1955–1978, reported at Posidonia (Fig. 1) are indicated by arrows in Fig. 4. Shorter term variations can be seen by direct examination of the record and commonly occur. Both presumably result from the interaction of climate (mainly wind) on the long, narrow body of water that forms the Gulf. Thus, if the earthquake was preceded by a period of high sea level, or was followed by a period of low sea level, reported coseismic changes could be exaggerated.

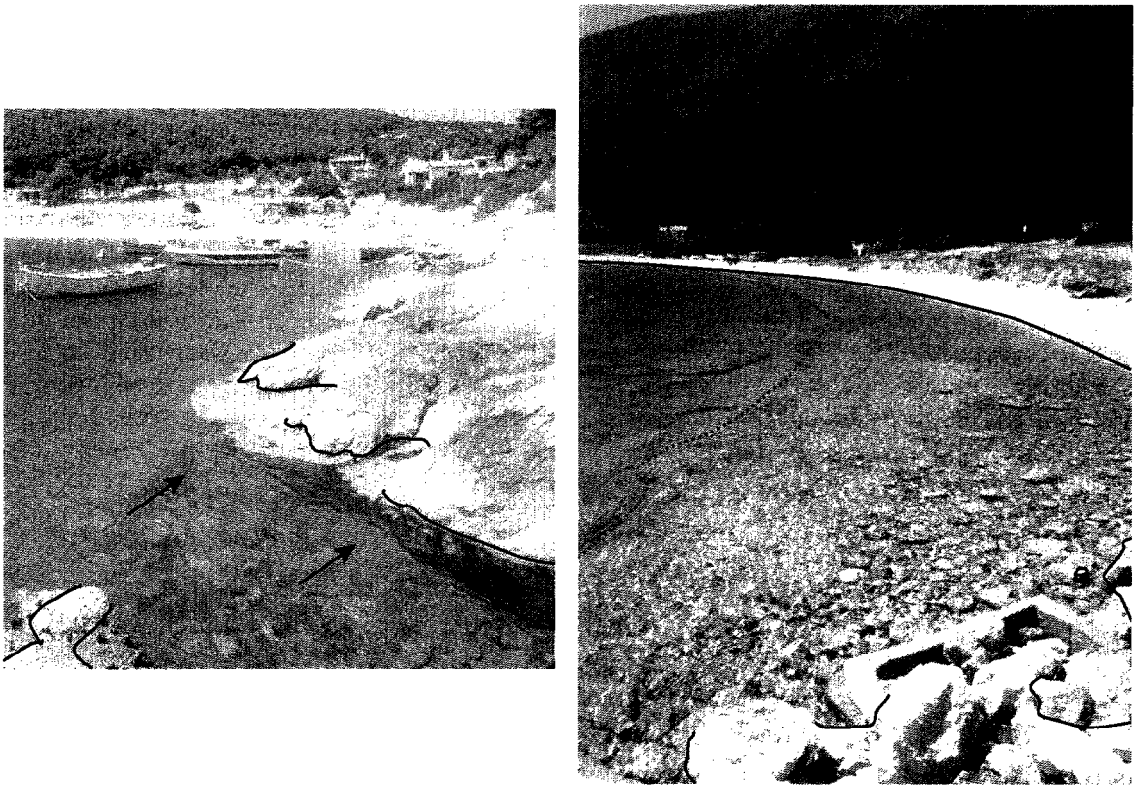

Fig. 2. Submergence of geological markers at Strava. Right: A beach submerged by the 1981 earthquakes. The approximate positions of mean sea level before the earthquake sequence and in 1993 when the photograph was taken are show by black lines. Left: Solution notch submerged by the 1981 earthquakes. The solution notch is indicated by arrows and the mean sea level in 1993, when the photograph was taken, is show by a black line.

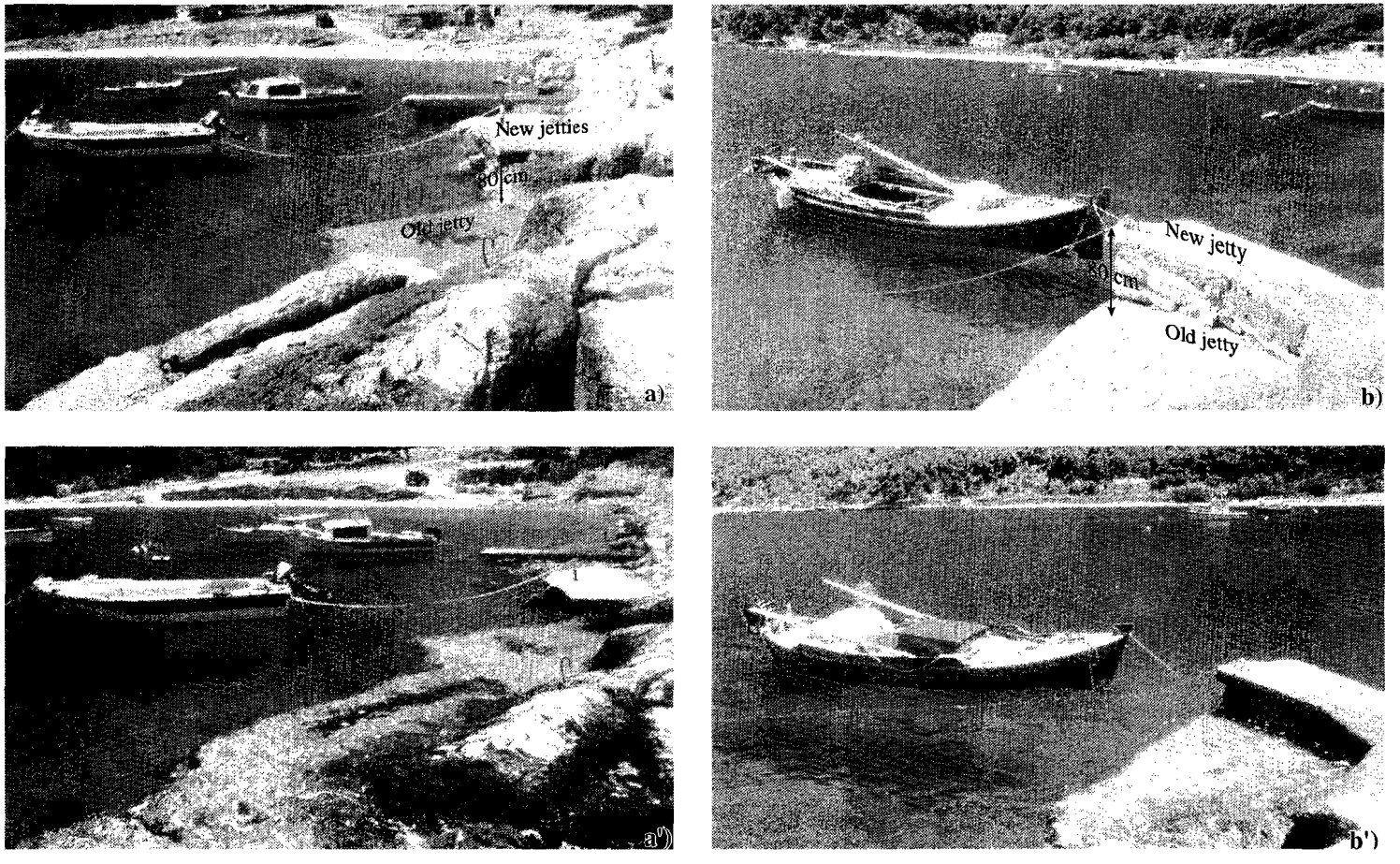

Fig. 3. Submergence of cultural markers at Strava Jetties down dropped by the earthquakes have been rebuilt 80 cm higher. This seems to provide a reliable measure of the sea level change over several years. The pairs of photographs of the same features (a and a') and (b and b') taken 3 days apart show that sea level can change by more than the lunar–solar tidal range would suggest.

Thus, although we refer to them, the reported values published by Vita-Finzi and King [7] must be treated with considerable caution, due to variation of the sea level and exaggeration by the local people who had recently suffered a catastrophe. Unlike such reports we regard the modifications to the height of the jetties at Strava to be inherently more reliable. They were rebuilt sometime after the earthquakes, and after sufficient time had elapsed for their owners to calmly assess what height change was needed to restore their original function. Overall, we conclude that the sea level change at Strava was closer to 80 cm than to the largest estimates of 1.5 m. However, we should note that a lapse of 10 years may be sufficient time [10] for significant isostatic rebound to have occurred. For 45° dipping normal faults the coseismic uplift to subsidence ratio is about 1:9 [11] whereas the completely isostatically relaxed ratio is about 1:3 [5]. If the immediately post-seismic subsidence was 95.4 cm, with an uplift of 10.6 cm, then complete relaxation would give a subsidence of 80 cm and an uplift of 26 cm. Thus the coseismic subsidence could have been about 1 m, but not as great as 1.5 m.

Examining the tidal record, it is possible to suggest that an uplift of about 8 cm was associated with the first two events at Posidonia; an observation that would be consistent with the later modelling. However, other variations of similar magnitude occur in the record (marked by an arrow A for example) and thus the observation is not robust. Nonetheless, nothing is visible in the tidal record to support the coseismic subsidence reported by Vita-Finzi and King [7] nearby at Loutraki.

3. Modelling the vertical displacements

The modelling that we carried out was based on assuming that the crust can be regarded as an elastic half-space, and the fault motion modelled as slip on a series of rectangular dislocation surfaces. This is achieved using the analytic results of Okada [12]. In the models, a Young's modulus of 70 GPa and a Poissons ratio of 0.25 are used. However, for a fixed fault slip, the displacement field models do not depend on modulus and are only mildly sensitive to Poissons ratio. Significant parameters concern only the geometry of the fault planes and their associated slip.

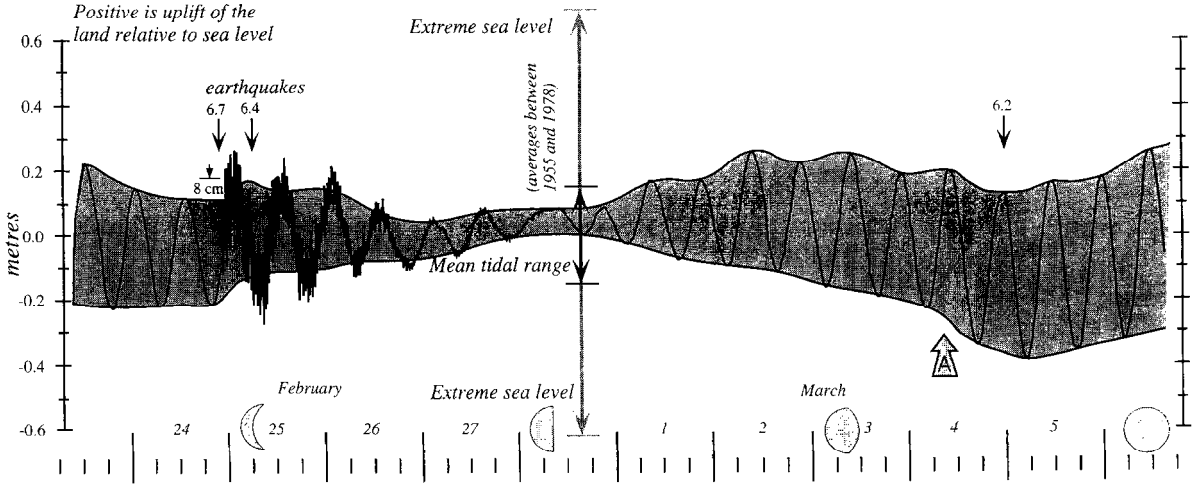

Fig. 4. Twelve days of tidal record from the tide gauge situated at Posidonia near to the Corinth Canal (from [19]). The times of the earthquakes are indicated. The first events created lowstands in the Gulf clearly visible in the record. The third event, for which the whole epicentral region was on land, did not. The mean tidal range and extreme sea levels for the period 1955–1978 are shown. It seems that the range can greatly exceed that caused by lunar and solar attraction alone. Even within the 12 day period significant fluctuations occur. A possible uplift of the land by about 8 cm may be associated with the first two events. However, similar change indicated by the arrow labelled A is not associated with an earthquake. The third event is not associated with observable uplift or subsidence.

Jackson et al. [1] reported surface fault dips that vary from 40° to 60° from geological data and the focal mechanisms suggest dips of 45 ± 5° [1,13,14]. We have adopted a dip of 50° for the planes of the first two events for which the best relocated hypocentres fall on the down-dip projection of the fault planes (Fig. 7).

King et al. [6] report aftershock hypocentres extending to a depth of 12–14 km, which presumably represents the base of the seismogenic layer. Bearing in mind that maximum slip in earthquakes appears to have diminished by this depth even if some slip extends to greater depth [15], we have chosen to model our events by a constant slip surface extending to a depth of 12 km. Our models are relatively insensitive to this choice of depth.

4. Results of the modelling

In the modelling we consider two possibilities. First, that the first event occurred on the offshore fault and the second produced all the surface rupture on the Perahora peninsula (Fig. 5). Second, that both of the events were responsible for the onshore rupture (Fig. 6).

Fig. 5a shows the case for motion occurring on a submarine fault with two segments of slightly different strike and a total length of 17 km. With the fault extending to 12 km depth this gives a down-dip width of 15.7 km which, for a moment of 8.8×10^{19} N · m, requires an average fault slip of 1.1 m. This gives a strain drop of 7.0×10^{-5}, equivalent to a stress drop of 21 bar.

If the fault slipped to a depth of 16 km (down-dip width of 20.9 km) this would produce a fault with a strange rectangular aspect ratio (the ratio of depth to fault length). Consequently, should the fault slip extend to that depth, it might be expected to extend further along strike; perhaps 20 km. Under these circumstances the strain drop would be 3.5×10^{-5} giving a low stress drop of 10.5 bar. Although possible, this seems unlikely. It slightly reduces the uplift at the end of the Perahora peninsula, but the change is so small that we do not show a separate model.

The second shock is regarded as having occurred on the two principal faults on the peninsula. The Pisia fault, 14 km in length, is given a displacement of 70 cm at the centre reducing at the ends to give an average slip of 42 cm. The Alephohori fault (13 km long) is given a average displacement of 20 cm. The combination is consistent with a moment of 4.0×10^{18} N · m. The associated strain drop is 2.0×10^{-5} N · m, equivalent to a low stress drop of 6 bar. If this scenario is correct, it seems impossible that the fault could have extended to greater depth. Not only would the stress drop become unusually small, but the predicted surface slip, already 50% of that observed, would reduce to 25%. To increase the stress drop while maintaining the same seismic moment would require the fault length to be decreased to a degree incompatible with the surface slip amplitude of the surface rupture. As we shall discus later, slip on the Alepohori fault apparently extends even further east than for this model. Distributing the slip over such a greater fault length would reduce the maximum slip and stress drop even more below likely values.

The model in Fig. 5a further requires that all of the subsidence at Strava and Skinos resulted from the second event and none from the first. The predicted values of subsidence are 25 and 40 cm, respectively. This is very much less than the immediate post-seismic estimates and still a factor of three less than the new estimates reported earlier in this paper. The model also predicts a modest uplift of 10 cm at the end of the Perahora peninsula where local people reported subsidence. Although these reports may be in error, such a large error seems unlikely, especially bearing in mind that the coast just south of the tip of the peninsula is well populated with numerous buildings close to the water's edge.

Seismic moment estimates (Table 1) show substantial variability and could be underestimated by a factor of two. Fig. 5b shows a displacement model with seismic moment doubled. Vertical displacements everywhere are doubled, together with a doubling of strain and stress drops. Such values are high but not impossible. The increased slip is more consistent with the observed surface rupture, but still fails to adequately explain the subsidence around Strava and Skinos. A further defect of the model is that the predicted uplift at the tip of the Perahora peninsula of 20 cm is even greater than before.

We therefore conclude that, provided we assume

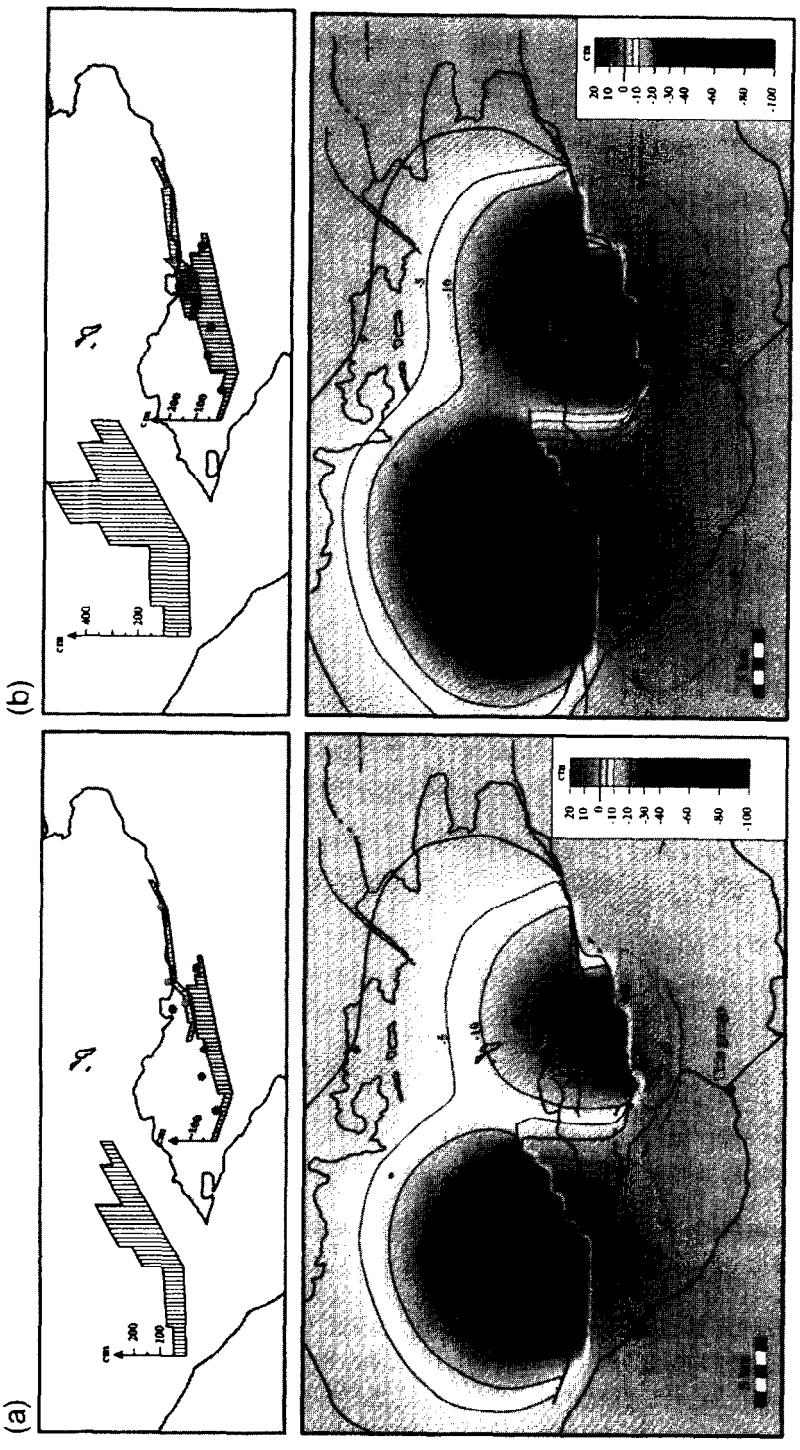

Fig. 5. Vertical displacements assuming that the first event (24th February) occurred on an offshore fault and the second event (25th February) reactivated the Perahora faults. In (a) fault slip has been adjusted to give seismic moments that are the mean of those shown in Table 1. In (b) all slip values are doubled to correspond to a doubling of the seismic moment for both events (see text). In the figures showing the distribution of slip on the faults, circles indicate values of observed surface slip.

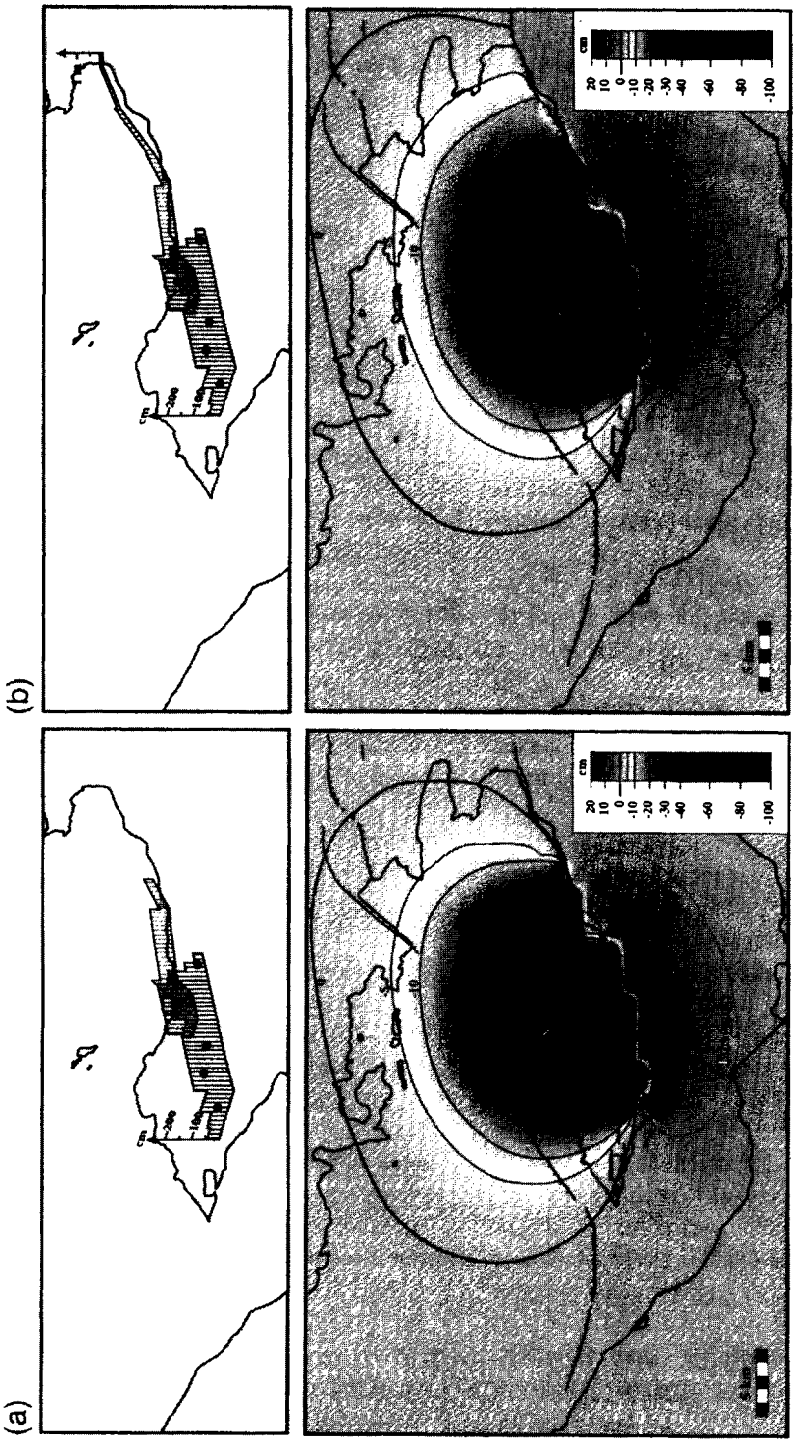

Fig. 6. Vertical displacements assuming that both the first (24th February) and second events (25th February) produced rupture on the Perahora peninsula. In (a) rupture is assumed to terminate west of Alepohori and in (b) it is permitted to extend to the eastern end of the Alepohori fault. In the figures showing the distribution of slip on the faults, circles indicate values of observed surface slip. The slip distribution used in (b) appears to explain the observed vertical motions best and is used for the Coulomb stress calculations shown in Fig. 7. As discussed in the text however, the exact geometry and slip on the eastern end of the Alepohori fault is poorly constrained.

that all of the surface rupture on the Perahora peninsula resulted from the second event alone, it is difficult to imagine any further modifications to the parameters that would create a displacement field consistent with the observations.

We now consider the case for which both of the events are regarded as contributing to rupture on the Perahora peninsula. In Fig. 6a the first shock is considered to have moved the Pisia fault. The fault is taken to be 14 km long with a displacement of 2.0 m at the centre, reducing at the ends to give an average slip of 1.3 m. This gives a strain drop of 9.0×10^{-5} and a stress drop of 27 bar. The second event is assumed to occur on the Alepohori fault, taken to have a length of 13 km, with a lower average displacement of 66 cm. There is reason to believe that motion on this fault in fact extended to the east of Alepohori itself. Unequivocal evidence of surface breaks is absent because of severe topography and landslides. However, some coastal uplift near Alepohori and subsidence and coastal inundation north of the eastern extremity of the fault suggest that motion occurred at depth, if not at the surface. In Fig. 6b slip is spread along 21 km of fault. This gives a strain drop of 2.6×10^{-5} and a stress drop of 8 bar.

Both models are more consistent with the observations. A slight subsidence is predicted at the end of the Perahora peninsula, and subsidence of 0.8 m and 1.2 m at Strava and Skinos, respectively, are consistent with the lower range of observations. The large values of subsidence further east on the northern coast of the Perahora peninsula reported by Vita-Finzi and King [7] are not predicted, but, as reported above, there is good reason to believe them to be in error. Uplift of about 7 cm is predicted near Loutraki where subsidence was reported (Fig. 1). However, an uplift of 5 cm at the nearby tide gauge station at Posidonia is consistent with observations.

The reliable observations are satisfactorily explained using the average values of seismic moment determined for the events (Table 1). Much lower values of seismic moment can be discounted because they would cause observed surface displacements to be less than those observed. Higher values are possible and could be adjusted to explain larger sea level changes at Strava [2], but a value of 1.5 m still seems too high. Such values would be associated with higher values of uplift at Posidonia. However, an uplift of 10 cm, which could be associated with a doubling of the fault slip, remains compatible with the tide gauge record.

From the foregoing models we conclude that motion due to both events is required to explain the surface faulting and the subsidence on the Perahora peninsula. The second event alone cannot produce sufficient displacement and subsidence of the coast. The requirement that both events must be associated with faulting on Perahora peninsula also precludes the possibility that the first event occurred on a south dipping antithetic fault, below sea level, on the northern side of the Gulf (Fig. 1).

5. Coulomb static stress modelling

The 1981 Corinth earthquake sequence propagated from southwest to northeast. To assess the influence of one earthquake on the next, we model the pattern of Coulomb static stress changes in half space [15–17]. In Fig. 7, the stress changes are shown calculated for an effective coefficient of friction of 0.4 at a depth of 6 km (the middle of the seismogenic zone) using the fault geometry and slip distribution that fits well with the uplift and subsidence observations (those used in Fig. 6b). In each figure the faults at the surface are shown in grey and in black their approximate location at depth from simple down dip projection.

Fig. 7a shows the stress changes due to the first event alone. Coulomb stresses are reduced north and south of the fault rupture and are increased at its ends. The best relocated hypocentres [3] fall on parts of the fault where the Coulomb stress was increased by more than 5 bar. Perhaps more significant than the location of the hypocentres is that much of the fault that ruptured falls in a region where stress increased by more than 3 bar, about 30% of the stress drop. Even at the eastern end of the fault, stress increased by 1 bar.

Fig. 7b shows the Coulomb stress change resulting from both the first and second shocks. The pattern of Coulomb stress change is more complicated than in Fig. 7a, mainly because of changes in strike of the fault rupture (from 45°N to 90°N). The slip decreases gradually from 30 cm to 10 cm at the eastern extremity of the fault rupture. The informa-

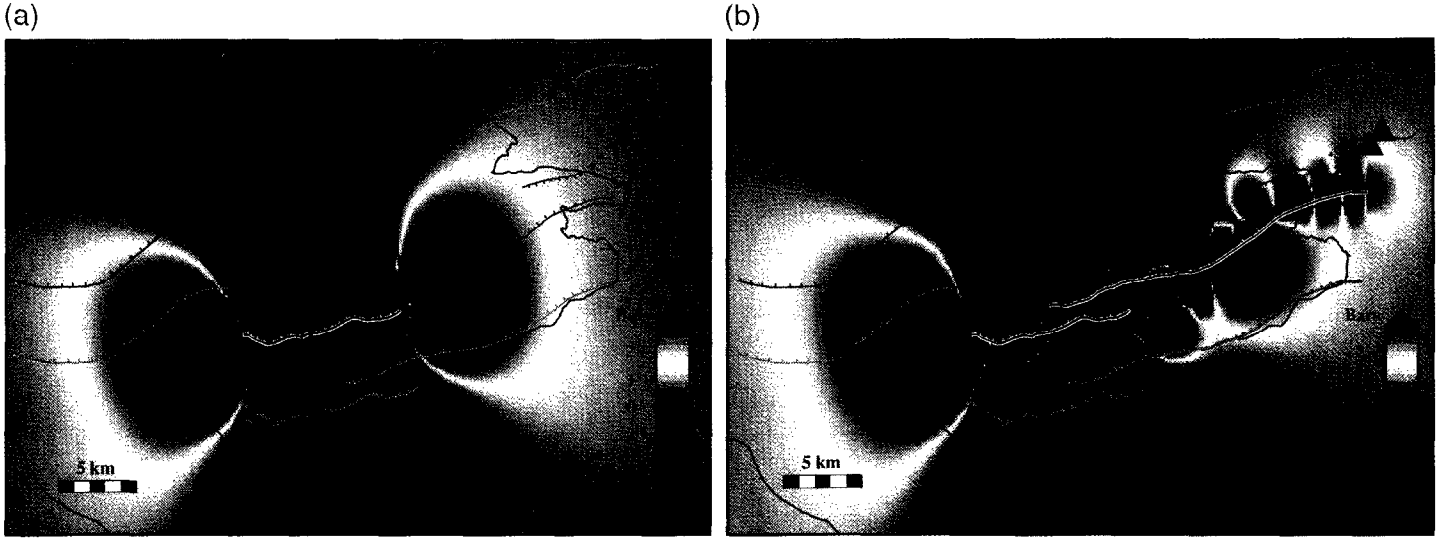

Fig. 7. (a) Coulomb stress changes at a depth of 6 km for normal faults striking parallel to the Alepohori fault. The fault slip distribution used is that for the Pisia fault shown in Fig. 6b. Rectangles indicate the best relocated hypocentres of the second shock [3]. (b) Coulomb stress changes at a depth of 6 km for faults striking parallel to the Kaparelli fault. The fault slip distribution used is that for the Pisia and Alepohori faults shown in Fig. 6b. Triangles indicate the best relocated hypocentres of the third shock [3]. In both figures the location of surface faults is indicated by grey lines and the estimated location at 6 km depth by black lines. The portion of the fault that has slipped is shown as black outlined by white.

tion we have about the geometry, or the slip distribution for the eastern Alepohori fault, and thus the stress distribution close to the fault, may be inexact. However, there is no doubt that significant changes of strike do exist and most probably where we show them. Whatever the detailed pattern near the fault may be, the more distant stress pattern and our overall interpretation of it should be unaffected.

The best relocated hypocentres [3] fall at the eastern end of the Kaparelli fault suggesting that rupture must then have progressed from east to west. However they fall in a lobe of stress increase of between 1 and 2 bar at the eastern end of the fault. Except for a short stretch, all of the Kaparelli fault was subject to a stress increase of greater than 1 bar, more than 6% of the stress drop of the third event. It is perhaps worth noting that the effect of rupture in the second event extending east of Alepohori (as in Fig. 6b) rather than terminating further to the west (as in Fig. 6a) is to reduce the amplitude of the Coulomb stress rise over the western part of the Kaparelli fault. This may explain why the Kaparelli event initiated at the eastern end of the faulting (see the epicentral location in Fig. 7b).

In Fig. 7 it can be seen that the first event raised the Coulomb stress for the offshore fault to the west as much as the increase that triggered the second shock to the east. However, an earthquake in 1928 (Mb 6.3) [18] probably occurred on this offshore fault leaving insufficient tectonic loading for even a substantial trigger stress to initiate further rupture.

6. Conclusions

Using elastic dislocations in a half space, we have modelled the vertical displacement field resulting from the 1981 earthquake sequence and compared it both with previously reported sea level changes and our own more recent observations. Within any plausible interpretation of the observations the short term and longer term sea level variation can be explained only if the first two shocks produced the surface rupture seen on the Perahora peninsula. The western offshore fault appears not to have been reactivated during the 1981 earthquake sequence, but was probably responsible for the destructive 1928 Corinth earthquake [18].

The foregoing interpretation is supported by simple modelling of Coulomb static stress changes to understand better the sequence of rupture propagation. We observe a close correspondence between the epicentral regions of the second and the third shocks and regions where Coulomb stresses increased by more than 1 bar as a result of previous fault slip. In the case of the second event, which occurred less than 4 h after the first, the triggering stress was a significant proportion (30%) of the final stress drop. For the third event, 7 days later, the increase was a more modest 6% of the stress drop. It therefore appears that, overall, the rupture propagated from southwest to northeast, with the second event tightly coupled to the first and the third event coupled to the first two, but less tightly. Rupture did not propagate to the east, probably because loading stress had been reduced by an event in 1928.

Where Coulomb stresses are increased we cannot in general know the degree to which hazard has been increased without further information about the earthquake history and, hence, the stress loading history of a region [15]. We have no direct evidence of the seismic history of the Perahora peninsula, but, unlike the offshore fault, a lack of recent events must have caused the faults to the east of the Pisia fault to be loaded before the first 1981 event occurred. Nonetheless, since the stress increase of several bars on the offshore fault is a substantial proportion of the likely stress drop in a future earthquake, its earthquake potential must have been substantially increased. ***[PT]***

References

[1] J.A. Jackson, J. Gagnepain, G. Houseman, G.C.P. King, P. Papadimitriou, C. Soufleris and J. Virieux, Seismicity, normal faulting and the geomorphological development of the Gulf of Corinth (Greece): the Corinth earthquakes of February and March 1981, Earth Planet. Sci. Lett. 57, 377–397, 1982.

[2] G.C.P. King, Z.X. Ouyang, P. Papadimitriou, A. Deschamps, J. Gagnepain, G. Houseman, J.A. Jackson, C. Soufleris and J. Virieux, The evolution of the Gulf of Corinth (Greece): an aftershock study of the 1981 earthquakes, Geophys. J.R. Astron. Soc. 80, 677–683, 1985.

[3] T. Taymaz, J.A. Jackson and D.P. McKenzie, Active tectonics of the north and central Aegean Sea, Geophys. J. Int. 106, 433–490, 1991.

[4] R.E. Abercrombie, I.G. Main, A. Douglas and P.W. Burton, The nucleation and rupture process of the 1981 gulf of Corinth earthquake from deconvolved broadband data, Geophys. J. Int., in press.
[5] R. Armijo, B. Meyer, G.C.P. King, D. Papanastassiou and A. Rigo, Quaternary evolution of the Corinth rift and its implications for the late Cenozoic evolution of the Aegean, J. Geophys. Int., in press.
[6] G.C.P. King, Photograph, EOS 66, cover, 1985.
[7] Vita-Finzi and G.C.P. King, The seismicity, geomorphology and structural evolution of the Corinth area of Greece, Philos. Trans. R. Soc. London 314, 379–407, 1985.
[8] S.G. Khoury, N.R. Tilford, U. Chandra and D. Amick, The effect of multiple events on isoseismal maps of the 1981 earthquake at the Gulf of Corinth, Bull. Seismol. Soc. Am. 73, 655–660, 1983.
[9] P.A. Pirazzoli, S.C. Stiros, M. Arnold, J. Laborel, F. Laborel-Deguen and S. Papageorgiou, Episodic uplift deduced from the holocene shoreline in the Perachora peninsula, Tectonophysics 229, 201–209, 1994.
[10] W. Thatcher, The earthquake deformation cycle, recurrence, and the time predictable model, J. Geophys. Res. 89, 5674–5680, 1984.
[11] G.C.P. King, R.S. Stein and J.B. Rundle, The growth of geological structures by repeated earthquakes 1. Conceptual framework, J. Geophys. Res. 93, 13307–13318, 1988.
[12] Y. Okada, Internal deformation due to shear and tensile fault in a half space, Bull. Seismol. Soc. Am. 82, 1018–1040, 1992.
[13] W.-Y. Kim and O. Kulhanek, Source processes of the 1981 Gulf of Corinth earthquake sequence from body-wave analysis, Bull. Seismol. Soc. Am. 74(2), 459–477, 1984.
[14] G. Ekström and P. England, Seismic strain rates in regions of distributed continental deformation, J. Geophys. Res. 94, 10,231–10,257, 1989.
[15] G.C.P. King, R.S. Stein and J. Lin, Static stress changes and the triggering of earthquakes, Bull. Seismol. Soc. Am. 84(3), 935–953, 1994.
[16] R. Stein, G.C.P. King and J. Lin, Change in failure stress on the southern San Andreas fault system caused by the 1992 magnitude = 7.4 Landers earthquake, Science 258, 1328–1332, 1992.
[17] R.S. Stein, G.C.P. King and J. Lin, Stress triggering of the 1994 M = 6.7 Northridge, California, earthquake by its predecessors, Science 265, 1432–1435, 1994.
[18] N.N. Ambraseys and J.A. Jackson, Seismicity and associated strain of central Greece between 1890 and 1988, Geophys. J. Int. 101, 663–708, 1990.
[19] C. Perissoriatis, D. Miropoulos and I. Angelopoulos, The role of the earthquake in inducing sediment mass movement in the eastern Korinthiakos gulf, an exemple from the February 24–March 4, 1981 activity, Mar. Geol. 55, 35–45, 1984.
[20] A.M. Diewonski and J.H. Woodhouse, An experiment in systematic study of global seismicity: centroid moment tensor for 201 moderate and large earthquakes of 1981, J. Geophys. Res. 88, 3247–3271, 1983.
[21] M. Bezzeghoud, A. Deschamps and R. Madariaga, Broadband modelling of the Corinth, Greece earthquake of February and March 1981, Ann. Geophys. 4, 301–314, 1986.